Journal of Computational Mathematics
Vol.29, No.1, 2011, 74–90.

http://www.global-sci.org/jcm
doi:10.4208/jcm.1004-m3195

HIGH-ORDER LOCAL ABSORBING BOUNDARY CONDITIONS FOR HEAT EQUATION IN UNBOUNDED DOMAINS*

Xiaonan Wu
Department of Mathematics, Hong Kong Baptist University, Kowloon, Hong Kong, China
Email: xwu@hkbu.edu.hk
Jiwei Zhang
Division of Mathematical Sciences, School of Physical and Mathematical Sciences, Nanyang Technological University, Singapore 637371, Singapore
Email: jwzhang@math.hkbu.edu.hk

Abstract

With the development of numerical methods the numerical computations require higher and higher accuracy. This paper is devoted to the high-order local absorbing boundary conditions (ABCs) for heat equation. We proved that the coupled system yields a stable problem between the obtained high-order local ABCs and the partial differential equation in the computational domain. This method has been used widely in wave propagation models only recently. We extend the spirit of the methodology to parabolic ones, which will become a basis to design the local ABCs for a class of nonlinear PDEs. Some numerical tests show that the new treatment is very efficient and tractable.

Mathematics subject classification: 65M06, 65M12, 65M15.
Key words: Heat equation, High-order method, Absorbing boundary conditions, Parabolic problems in unbounded domains.

1. Introduction

Heat equation rises from many fields, for examples, the heat transfer, fluid dynamics, astrophysics, finance or other areas of applied mathematics. In this paper, we consider the numerical solutions of heat equation on unbounded spatial domains. A real challenge is the unboundedness of the physical domains, the traditional methods (finite element method and finite difference method) can not be used in a straight forward manner. Therefore, many mathematicians, engineers and physicists are attracted and devoted to the study of these problems. In the early literatures, Givoli [8] studied the heat problems on unbounded domains, in which the author tried to get DtN artificial boundary condition on the given artificial boundary. Greengard and Lin [11] developed a new algorithm for solving the heat problem on unbounded domains, the algorithm was based on the evolution of the continuous spectrum of the solution. Li and Greengard [25] also proposed a fast solver for heat equation in free space. Strain [29] presented efficient and accurate new adaptive methods related to the fast Gauss transform. Han and Huang [18, 19] presented an exact artificial boundary condition to reduce the original heat equation to an initial-boundary-value problem on a finite computational domain. Wu and Sun [32] constructed a finite difference scheme for one-dimensional case and proved that the scheme was uniquely solvable, unconditionally stable and convergent with the order two in space and the order 3/2 in time under an energy norm. Zheng [41] considered the approximation,

* Received August 19, 2009 / Revised version received December 3, 2009 / Accepted January 20, 2010 / Published online September 20, 2010 /

stability and fast evaluation of 1-D heat equation. Han and Yin [22] presented the numerical solution of 3-D parabolic problems.

The ABCs include the global ABCs and local ABCs. The global ABCs are usually the natural integral equation, i.e., DtN mapping and hence, lead to the well-approximation and well-posed truncated problems, but the implementation cost is expensive. For a great details one can refer to [1, 3, 7, 12, 14, 17, 20, 21, 23, 33, 34, 36, 39, 40, 42] and references therein. On the other hand, local ABCs are computationally efficient, but the accuracy and stability are the main concerns. Enquist and Majda [6] proposed a whole family of local boundary conditions for wave equation, which not only resulted in stable difference approximation, but also minimized the unphysical reflections.

For long time simulation or when the mesh size is small enough, it needs to increase the order of the local ABCs. The high-order method has been used in wave propagation models [5, 27, 28, 30, 31]. Works in [6, 26] suggested the higher-order paraxial approximation as artificial boundary conditions. Based on the use of auxiliary functions, [2] proposed a family of paraxial wave equation approximation, and Collino developed the high-order ABCs for the 2-D wave equation and gave the boundary conditions at corners. Givoli et al [9, 10] proposed a new high-order ABCs for time-dependent wave problems in unbounded domains. More works and their extensions [13, 15, 16], associated with ABCs, improved the work of the Givoli-Neta in some respects (accuracy and stability).

Recently, Zhang, Xu and Wu [37, 38], proposed a novel unified approach to design the local ABCs for nonlinear Schrödinger equation. Based on the well-known operator-splitting method, the procedure of unified approach is to approximate the linear subproblem by distinguishing the incoming and outgoing wave; then unite the resulting approximate operator and the nonlinear subproblem to obtain nonlinear boundary conditions. Brunner, Wu and Zhang [4] successfully applied the method to semilinear parabolic equation on unbounded spatial domain, where the design of local ABCs plays an important role to get the suitable approximate operator for heat equation. In this paper we extend the spirit of the high-order methodology to constructing high-order ABCs for heat equations, and prove that the resulting ABCs are stable. By applying Laplace and Fourier transforms and their inverse transforms, we approximate the one-way equation to obtain the high-order boundary conditions by padé polynomial at expansion point z_0, and introduce the specially defined auxiliary variables to avoid the high derivatives beyond order two, which make the formula tractable when N is chosen larger.

The brief description of this paper is as follows. Section 2 is devoted to the construction of high-order ABCs. In Section 3 the focus of the presentation is on the stability analysis for the reduced initial-boundary-value problems. In Section 4 some numerical examples show the tractability and effectiveness of the high-order ABCs. We end the paper with some concluding remarks.

2. Design of High-Order Absorbing Boundary Conditions

Denote the spatial coordinate by $\mathbf{x}$, which for one-dimensional case is $\mathbf{x} = x$, two-dimensional case is $\mathbf{x} = (x, y)$, and three-dimensional case is $\mathbf{x} = (x, y, z)$. Denote the infinity domain by Ω, the computational domain by Ω_i, the boundary by $\Gamma = \partial\Omega$, and the exterior domain by $\Omega_e = \Omega \setminus \Omega_i$. Heat equation can be written as follows:

$$u_t = a^2 \Delta u + f(\mathbf{x}, t), \qquad \text{in } \Omega,\ t > 0, \tag{2.1}$$

$$u(\mathbf{x},0) = u^0, \tag{2.2}$$
$$u(\mathbf{x},t)|_\Gamma = g, \tag{2.3}$$
$$u \to 0, \qquad \text{as } |\mathbf{x}| \to +\infty, \tag{2.4}$$

where the source term f($\mathbf{x}$,t) and initial value u^0 are compactly supported functions, and vanish outside $B_0 = \{\mathbf{x} : |\mathbf{x}| < r\}$, namely,

$$\text{supp}\{f(\mathbf{x},t)\} \subset B_0 \times [0,T],\ \text{supp}\{u^0(\mathbf{x})\} \subset B_0.$$

2.1. One-dimensional case

To provide the spirit of the high-order ABCs, we restrict the problem (2.1)-(2.4) on the exterior domain Ω_e, the solution $u(x,t)$ satisfies:

$$u_t - a^2 u_{xx} = 0, \qquad (x,t) \in \Omega_e; \tag{2.5}$$
$$u(x,0) = 0, \tag{2.6}$$
$$u\big|_{x=x_l} = u(x_l,t), \qquad u\big|_{x=x_r} = u(x_r,t), \tag{2.7}$$
$$u \to 0, \qquad \text{as } |\mathbf{x}| \to \infty. \tag{2.8}$$

Applying Laplace transformation with respect to t, we have

$$s\tilde{u} - a^2 \tilde{u}_{xx} = 0, \tag{2.9}$$

where the Laplace transformation is given as

$$\widetilde{u}(x,s) = \int_0^\infty e^{-st} u(x,t)dt. \tag{2.10}$$

The equation (2.9) is homogeneous and has two linearly independent solutions. The first solution $\widetilde{u}^{(1)}(x)$ vanishes and the second solution $\widetilde{u}^{(2)}(x)$ grows to infinity as $x \to +\infty$. It is obvious that condition (2.8) can be satisfied if and only if the growing solution $\widetilde{u}^{(2)}(x) = e^{x\sqrt{s/a^2}}$ does not contribute to the solution $\widetilde{u}(x)$ of (2.9) in the semi-infinite interval $[x_r, +\infty)$. Hence we give up the growing solution and accept the decaying one $\widetilde{u}^{(1)}(x) = e^{-x\sqrt{s/a^2}}$, which is equivalent to the following homogeneous relations:

$$\partial_x \widetilde{u} \pm \sqrt{\frac{s}{a^2}}\tilde{u} = 0, \tag{2.11}$$

where the plus sign in "$\pm$" corresponds to the right boundary conditions at x_r, and the minus sign to the left boundary conditions at x_l. By using $\sqrt{s} = \frac{s}{\sqrt{s}}$ and the following formula

$$\mathcal{L}^{-1}\left\{\frac{1}{\sqrt{s+\alpha}}\right\} = \frac{1}{\sqrt{\pi t}} e^{-\alpha t}, \tag{2.12}$$

from Eq. (2.11) we have the exact ABC at the artificial boundaries:

$$\partial_x u \pm \sqrt{\frac{1}{a^2 \pi}} \int_0^t \frac{1}{\sqrt{t-\tau}} \frac{\partial u}{\partial \tau} d\tau = 0, \tag{2.13}$$

which is global in time. Now we consider the construction of the high-order local ABCs. In formula (2.11), we denote $z = \frac{s}{a^2}$ and expand the irrational function $\sqrt{z}$ by using the Padé approximation:

$$\sqrt{z_0}\sqrt{\frac{z}{z_0}} = \sqrt{z_0}\sqrt{1-\left(1-\frac{z}{z_0}\right)} \approx \sqrt{z_0} - \sqrt{z_0}\sum_{k=1}^{N}\frac{b_k\left(1-\frac{z}{z_0}\right)}{1-a_k\left(1-\frac{z}{z_0}\right)}, \tag{2.14}$$

where

$$a_k = \cos^2\left(\frac{k\pi}{2N+1}\right), \quad b_k = \frac{2}{2N+1}\sin^2\left(\frac{k\pi}{2N+1}\right), \qquad k = 1, \cdots, N.$$

The parameter z_0 plays the role of the expansion point in the approximation (2.14). Fig. 2.1 shows that the expansion (2.14) at $z_0 = 1.0$ can approximate the irrational function quickly with the truncated number N increasing.

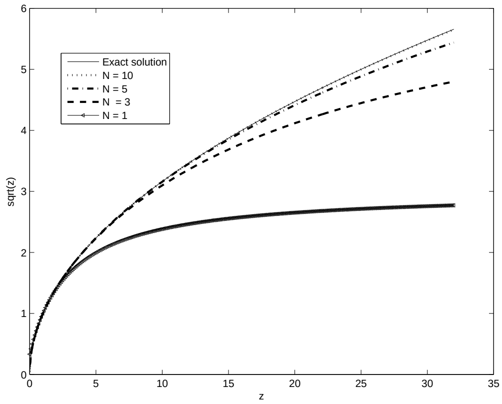

Fig. 2.1. The Padé approximation to the $\sqrt{z}$ with different N and z_0.

We substitute the approximation (2.14) into (2.11) to obtain

$$\partial_x\tilde{u} \pm \left(\sqrt{z_0} - \sqrt{z_0}\sum_{k=1}^{N}\frac{b_k\left(1-\frac{z}{z_0}\right)}{1-a_k\left(1-\frac{z}{z_0}\right)}\right)\tilde{u} = 0. \tag{2.15}$$

For a simple case, we first choose $N = 1$ and substitute $z = s/a^2$ to obtain

$$(1-a_1)z_0\partial_x\tilde{u} + \frac{a_1 s}{a^2}\partial_x\tilde{u} \pm (1-a_1-b_1)z_0\sqrt{z_0}\tilde{u} \pm \frac{(a_1+b_1)\sqrt{z_0}s}{a^2}\tilde{u} = 0. \tag{2.16}$$

Applying the inverse Laplace transformation, we have

$$3z_0\partial_x u + \frac{1}{a^2}\partial_x\partial_t u \pm z_0\sqrt{z_0}u \pm \frac{3\sqrt{z_0}}{a^2}\partial_t u = 0. \tag{2.17}$$

It is easy to see that the partial derivatives with respect to time increase with the truncated number N growing. This kind of high-order derivatives would bring us in a lot of trouble. Naturally the auxiliary variables are introduced to overcome the above disadvantages. Let

$$\begin{cases} \partial_x\tilde{u} - \sqrt{z_0}\tilde{u} + \sqrt{z_0}\sum\limits_{k=1}^{N} b_k\tilde{\varphi}_k = 0, & x = x_l, \\ (z_0 - a_k z_0 + a_k z)\tilde{\varphi}_k = (z_0 - z)\tilde{u}, & k = 1, \cdots, N, \end{cases} \tag{2.18}$$

$$\begin{cases} \partial_x \widetilde{u} + \sqrt{z_0}\widetilde{u} - \sqrt{z_0}\sum\limits_{k=1}^{N} b_k \widetilde{w}_k = 0, & x = x_r, \\ (z_0 - a_k z_0 + a_k z)\widetilde{w}_k = (z_0 - z)\widetilde{u}, & k = 1, \cdots, N. \end{cases} \tag{2.19}$$

After using the inverse Laplace transform to Eqs. (2.18)-(2.19) and, coupling the results with the heat equation, we have the reduced initial-boundary-value problems

$$\begin{cases} u_t = a^2 u_{xx} + f(x,t) & \text{in } \Omega_i, t > 0, \\ u(x,0) = u^0, & \\ \partial_x u + \sqrt{z_0}u - \sqrt{z_0}\sum\limits_{k=1}^{N} b_k w_k = 0, & x = x_r, \\ (1-a_k)z_0 w_k + a_k \dfrac{1}{a^2}\partial_t w_k = z_0 u - \dfrac{1}{a^2}\partial_t u, & k = 1, \cdots, N, \\ \partial_x u - \sqrt{z_0}u + \sqrt{z_0}\sum\limits_{k=1}^{N} b_k \varphi_k = 0, & x = x_l, \\ (1-a_k)z_0 \varphi_k + a_k \dfrac{1}{a^2}\partial_t \varphi_k = z_0 u - \dfrac{1}{a^2}\partial_t u, & k = 1, \cdots, N. \end{cases} \tag{2.20}$$

Eq. (2.20) implies the ABCs of order N. It does not involve high-order derivatives beyond the first-order and has no spacial derivatives for any auxiliary variable w_k or φ_k. Therefore, the auxiliary variables appear only at the artificial boundary point.

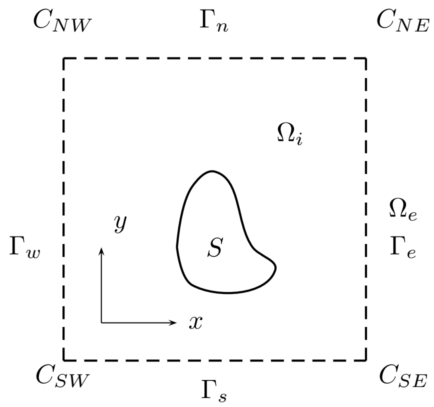

Fig. 2.2. Settings of unbounded problems.

2.2. High-dimensional cases

We have obtained the high-order ABCs for 1D spatial domain, which motivates us to apply the spirit to multi-dimensional cases. Without loss of generality, we only discuss the two-dimensional case, this idea can be easily extended to higher-dimensional cases. One of typical settings for problems in unbounded domains [10] is the exterior problem (Fig. 2.2). Let us firstly consider the problem (2.1)-(2.4) in the unbounded domain Ω_e:

$$u_t = a^2 \triangle u, \qquad \mathbf{x} \in \Omega_e, \tag{2.21}$$

$$u(\mathbf{x}, 0) = 0, \tag{2.22}$$

$$u|_{\Gamma_0} = u_1(y,t), \tag{2.23}$$

$$u|_{\Gamma} = g, \tag{2.24}$$

where the exterior domain $\Omega_e = \{\mathbf{x} : x \in (r,\infty), y \in (-\infty,\infty), t \in (0,T]\}$, the artificial boundary $\Gamma_0 = \{\mathbf{x} : x = r, y \in (-\infty,\infty)\}$. Problem (2.21)-(2.24) is not a well-posed problem since $u_1(y,t)$ is an unknown function. Applying Fourier transformation with respect to y and Laplace transformation to t, we have:

$$s\widetilde{\widehat{u}} = a^2\left(\widetilde{\widehat{u}}_{xx} - \eta^2\widetilde{\widehat{u}}\right), \tag{2.25}$$

where the Fourier transform is

$$\widehat{u}(x,\eta,t) = \int_{-\infty}^{+\infty} u(x,y,t)e^{-i\eta y}dy,$$

and the Laplace transform is the same as (2.10). The Eq. (2.25) is equal to

$$\widetilde{\widehat{u}}_{xx} - \left(\eta^2 + \frac{s}{a^2}\right)\widetilde{\widehat{u}} = 0, \tag{2.26}$$

and has two linearly independent solutions

$$\widetilde{\widehat{u}}^{(1)}(x) = e^{-x\sqrt{\eta^2+s/a^2}}, \qquad \widetilde{\widehat{u}}^{(2)}(x) = e^{x\sqrt{\eta^2+s/a^2}}.$$

Thus we have the general solution of Eq. (2.26) on the right boundary

$$\widetilde{\widehat{u}}(x,\eta,\zeta,s) = c_1e^{-x\sqrt{\eta^2+s/a^2}}. \tag{2.27}$$

Differentiate solution (2.27) with respect x and substitute (2.27) into the result. We obtain

$$\partial_x\widetilde{\widehat{u}} + \sqrt{\eta^2 + \frac{s}{a^2}}\widetilde{\widehat{u}} = 0. \tag{2.28}$$

Let $z = \eta^2 + s/a^2$ and substitute the expansion (2.14) into (2.28). We have

$$\partial_x\widetilde{\widehat{u}} + \sqrt{z_0}\widetilde{\widehat{u}} - \sqrt{z_0}\sum_{k=1}^{N}\frac{b_k(z_0-z)}{z_0 - a_k(z_0-z)}\widetilde{\widehat{u}} = 0. \tag{2.29}$$

For special case $N = 1$, we get

$$(1-a_1)\,z_0\partial_x\widetilde{\widehat{u}} + a_1\left(\eta^2 + \frac{s}{a^2}\right)\partial_x\widetilde{\widehat{u}} + (1-a_1-b_1)\sqrt{z_0}z_0\widetilde{\widehat{u}} + (a_1+b_1)\sqrt{z_0}\left(\eta^2 + \frac{s}{a^2}\right)\widetilde{\widehat{u}} = 0. \tag{2.30}$$

After the inverse Laplace and Fourier transforms, we obtain

$$3z_0\partial_x u + \partial_x\partial_y\partial_y u + \frac{1}{a^2}\partial_x\partial_t u + \sqrt{z_0}z_0 u - 3\sqrt{z_0}\partial_y\partial_y u - \frac{3}{a^2}\sqrt{z_0}\partial_t u = 0. \tag{2.31}$$

Clearly, the derivatives increase as the truncated number N increases, and the calculations become tedious. To avoid this difficulty, we introduce the auxiliary variables

$$\widetilde{\widehat{w}}_k = \frac{z_0 - z}{z_0 - a_k(z_0-z)}\widetilde{\widehat{u}}. \tag{2.32}$$

Then the approximation (2.29) is reduced to

$$\begin{cases} \partial_x\widetilde{\widehat{u}} + \sqrt{z_0}\widetilde{\widehat{u}} - \sqrt{z_0}\sum\limits_{k=1}^{N} b_k\widetilde{\widehat{w}}_k = 0, \\ (z_0 - a_kz_0 + a_kz)\widetilde{\widehat{w}}_k = (z_0 - z)\widetilde{\widehat{u}}, \qquad k = 1,\cdots,N. \end{cases} \tag{2.33}$$

Taking the inverse Fourier and Laplace transforms for (2.33), the original problem is reduced to the following approximation problem:

$$\begin{cases} u_t = a^2\Delta u + f(\mathbf{x},t) & \text{in } \Omega_i, t>0, \\ u(\mathbf{x},0) = u^0, \\ u(\mathbf{x},t)|_\Gamma = g, \\ \partial_x u + \sqrt{z_0}u - \sqrt{z_0}\sum\limits_{k=1}^{N} b_k w_k = 0, & \text{on } \Gamma_0, \\ (1-a_k)\, z_0 w_k + a_k\left(\frac{1}{a^2}\partial_t w_k - \partial_y\partial_y w_k\right) = z_0 u - \left(\frac{1}{a^2}\partial_t u - \partial_y\partial_y u\right), & k=1,\cdots,N. \end{cases} \tag{2.34}$$

Note that each auxiliary variable needs the datum at the two corner points, we deal with them as

$$\sqrt{z_0}b_n w_n = \alpha_n(\partial_x u + \sqrt{z_0}u), \qquad n = 1,\cdots,N,$$

where $\sum_{n=1}^N \alpha_n = 1$. Here we choose $\alpha_n = 1/N$. One can find that the values u at the corner points are equal to the boundary values g at the corner points.

Remark 2.1. It can be seen from the above derivation that high-order boundary conditions for three-dimensional case can be obtained by adding the derivative on the z direction in the fifth equation of (2.34). Furthermore, we can obtain the corresponding ABCs at other sides. Thus some corner boundary conditions are needed to decouple the ABCs together.

Now let us consider the 2-D heat problem (with $a = 1$ without loss of generality) on the exterior domain. Based on the Fourier transform and Laplace transform, we have the dispersion relation

$$s + \xi^2 + \eta^2 = 0. \tag{2.35}$$

By using the conditions $u(x,t) \to 0$ $(|x| \to \infty)$, the following dispersion relations can be obtained on the east and west artificial boundaries

$$-i\xi \pm \sqrt{s+\eta^2} = 0, \tag{2.36}$$

where the plus sign in "$\pm$" stands for the positive direction, and the minus for the negative direction. Take $z = \eta^2 + s$ and expand $\sqrt{z}$ in formula (2.14) with $N = 1$, substitute the result into Eq. (2.36) and solve the obtained algebraic equation, we have

$$s = -\frac{-i\xi\eta^2 \pm 3\sqrt{\xi_0}\eta^2 - 3i\xi_0\xi - \sqrt{\xi_0}\xi_0}{-i\xi \pm 3\sqrt{\xi_0}}. \tag{2.37}$$

Similarly, we can obtain the dispersion relation at the northern and southern boundaries

$$s = -\frac{-i\xi^2\eta \pm 3\sqrt{\xi_0}\xi^2 - 3i\eta_0\eta - \sqrt{\eta_0}\eta_0}{-i\eta \pm 3\sqrt{\eta_0}}. \tag{2.38}$$

Generally speaking, it is difficulty to obtain the suitable ABCs at corner points. We observe that the approximation in Eq. (2.16) corresponds to the (1,1)-Padé approximation to absorb the heat flow from the interior domain. Hence, for corners we use the (1,1)-Padé approximation to expand ξ^2 and η^2 with the expansion point (ξ_0, η_0). At the northern-eastern (C_{NE}) and southern-western (C_{SW}) corners, we have the algebraic equation

$$s = -\xi_0\frac{-3i\xi \pm \sqrt{\xi_0}}{-i\xi \pm 3\sqrt{\xi_0}} - \eta_0\frac{-3i\eta \pm \sqrt{\eta_0}}{-i\eta \pm 3\sqrt{\eta_0}}. \tag{2.39}$$

At northern-western (C_{NW}) and southern-eastern (C_{SE}) corners, the equations are given by

$$s = -\xi_0 \frac{-3i\xi - \sqrt{\xi_0}}{-i\xi - 3\sqrt{\xi_0}} - \eta_0 \frac{-3i\eta + \sqrt{\eta_0}}{-i\eta + 3\sqrt{\eta_0}}, \tag{2.40}$$

and

$$s = -\xi_0 \frac{-3i\xi + \sqrt{\xi_0}}{-i\xi + 3\sqrt{\xi_0}} - \eta_0 \frac{-3i\eta - \sqrt{\eta_0}}{-i\eta - 3\sqrt{\eta_0}}, \tag{2.41}$$

respectively. Following the duality of $s \leftrightarrow \partial_t, -i\xi \leftrightarrow \partial_x$ and $-i\eta \leftrightarrow \partial_y$, the corresponding local ABCs can be obtained: on Γ_e and Γ_w

$$3\xi_0 \partial_x u - \partial_x \partial_y^2 u + \partial_x \partial_t u \pm \sqrt{\xi_0} \left(\xi_0 u + 3\partial_t u - 3\partial_y^2 u \right) = 0; \tag{2.42}$$

on Γ_n and Γ_s

$$3\eta_0 \partial_y u - \partial_y \partial_x^2 u + \partial_t \partial_y u \pm \sqrt{\eta_0} \left(\eta_0 u + 3\partial_t u - 3\sqrt{\eta_0} \partial_x^2 u \right) = 0; \tag{2.43}$$

at C_{NE} and C_{SW}

$$\begin{aligned} &\partial_t \partial_x \partial_y u + (3\xi_0 + 3\eta_0) \partial_x \partial_y u \pm 3\sqrt{\xi_0} \partial_t \partial_y \pm 3\sqrt{\eta_0} \partial_t \partial_x u + 9\sqrt{\xi_0 \eta_0} \partial_t u \\ &\qquad \pm \sqrt{\eta_0}(9\xi_0 + \eta_0) \partial_x u \pm \sqrt{\xi_0}(9\eta_0 + \xi_0) \partial_y u + 3\sqrt{\xi_0 \eta_0}(\xi_0 + \eta_0) u = 0; \end{aligned} \tag{2.44}$$

at C_{NW} and C_{SE}

$$\begin{aligned} &\partial_t \partial_x \partial_y u + (3\xi_0 + 3\eta_0) \partial_x \partial_y u \pm 3\sqrt{\xi_0} \partial_t \partial_x \pm \sqrt{\xi_0}(9\eta_0 + \xi_0) \partial_x u - 9\sqrt{\xi_0 \eta_0} \partial_t u \\ &\qquad 3\sqrt{\xi_0 \eta_0}(\xi_0 + \eta_0) u = \pm 3\sqrt{\eta_0} \partial_t \partial_y u \pm \sqrt{\eta_0}(9\xi_0 + \eta_0) \partial_y u. \end{aligned} \tag{2.45}$$

Thus we are successful to design the corresponding local ABCs at boundaries and corners, which are the special case of high-order boundary conditions with $N = 1$. But the arbitrary high-order approximation at corners is still not solved. The obtained third-order local ABCs play an important role in designing the corresponding local ABCs for some nonlinear problems, e.g., semilinear parabolic problems with blow-up solutions on unbounded spatial domains [4].

3. Stability Analysis

In this section we consider the stability of the reduced initial-boundary-value problems.

3.1. One-dimensional case

Firstly, we prove the stability of the systems (2.20). Denote notation $||\cdot||_\Omega$ the usual norm in the Banach space $W^{m,p}(\Omega)$ with $m = 0$ and $p = 2$ and introduce the **Gronwall′s Lemma** (refer to [24]):

Lemma 3.1. *Suppose that $y \in C^1[0,T]$ and $\psi \in C[0,T]$ satisfy*

$$y'(t) \le cy(t) + \psi(t), \qquad 0 \le t \le T,$$

for some $c \ge 0$. Then

$$y(t) \le e^{ct} \left\{ y(0) + \int_0^t |\psi(\tau)| d\tau \right\}, \qquad 0 \le t \le T.$$

The stability of problem (2.20) is given by the following theorem.

Theorem 3.1. *Assume that the initial values are smooth enough. Then the Cauchy problem* (2.20) *has a unique weak solution and the energy estimate holds:*

$$||u||^2_{\Omega_i\times[0,t]} \le e^t \left(||u^0||_{\Omega_i} + \int_0^t \phi(\tau)d\tau \right), \tag{3.1}$$

where

$$\phi(t) = ||u^0||^2_{\Omega_i} + ||f||^2_{\Omega_i\times[0,t]}. \tag{3.2}$$

Proof. The unique solution follows from the energy estimate. Here we focus on the energy estimate based on the Galerkin method.

(i) Multiply the first equation in (2.20) by u, and integrate the result by part over $\Omega_i \times [0,t]$, we arrive at

$$\begin{aligned}&\frac{1}{2}||u||^2_{\Omega_i} + a^2||u_x||^2_{\Omega_i\times[0,t]}\\ =&\frac{1}{2}||u^0||^2_{\Omega_i} + a^2\int_0^t u(r,t)u_x(r,t)dt - a^2\int_0^t u(l,t)u_x(l,t)dt + \int_0^t\int_{\Omega_i} fudxdt.\end{aligned} \tag{3.3}$$

(ii) Multiply the third equation of (2.20) by u and integrate from 0 to t, we have

$$\int_0^t u(r,t)u_x(r,t)dt + \sqrt{z_0}\int_0^t u^2(r,t)dt - \sqrt{z_0}\sum_{k=1}^N b_k \int_0^t w_k(t)u(r,t)dt = 0. \tag{3.4}$$

(iii) Multiply the forth equation of (2.20) by $a_k w_k(t) + u(r,t)$ and integrate from 0 to t, we obtain

$$\begin{aligned}a^2\int_0^t a_k(1-a_k)z_0 w_k^2(t)dt+&\frac{1}{2}\Big(a_k w_k(t) + u(r,t)\Big)^2 - \frac{1}{2}\Big(a_k w_k^0 + u^0(r)\Big)^2\\ &+ a^2\int_0^t (1-2a_k)z_0 w_k(t)u(r,t)dt - a^2\int_0^t z_0 u^2(r,t)dt = 0.\end{aligned} \tag{3.5}$$

(iv) Noting that u^0 is a smooth function with compact support, the initial data u^0 and w_k^0 vanish at the artificial boundary, we multiply (3.5) by b_k and sum the resulting identities from 1 to N to have

$$\begin{aligned}&a^2\sum_{k=1}^N\int_0^t b_k a_k(1-a_k)z_0 w_k^2(t)dt + \sum_{k=1}^N \frac{1}{2} b_k(a_k w_k(t) + u(r,t))^2\\ &+ a^2\sum_{k=1}^N\int_0^t b_k(1-2a_k)z_0 w_k(t)u(r,t)dt - a^2\sum_{k=1}^N\int_0^t b_k z_0 u^2(r,t)dt = 0.\end{aligned} \tag{3.6}$$

By the same argument, we can obtain the corresponding equations at the left artificial boundary, which are similar to (3.4) and (3.6).

(v) Combining (3.3), (3.4), (3.6) and the corresponding equations at $x = x_l$ yields

$$\begin{aligned}
&\frac{1}{2}||u||^2_{\Omega_i} + a^2||u_x||^2_{\Omega_i\times[0,t]} + \frac{1}{2}\sum_{k=1}^{N}\frac{b_k}{\sqrt{z_0}}\left[\left(a_k w_k(t) + u(r,t)\right)^2 + \left(a_k\varphi_k(t) + u(l,t)\right)^2\right] \\
=&\frac{1}{2}||u^0||^2_{\Omega_i} - a^2\sqrt{z_0}\left(1 - \sum_{k=1}^{N} b_k\right)\left(||u(r,t)||^2_{[0,t]} + ||u(l,t)||^2_{[0,t]}\right) \\
&\quad - a^2\sqrt{z_0}\sum_{k=1}^{N} b_k a_k(1-a_k)\left(||w_k(t)||^2_{[0,t]} + ||\varphi_k(t)||^2_{[0,t]}\right) \\
&\quad + a^2\sqrt{z_0}\sum_{k=1}^{N}\int_0^t 2b_k a_k\left(w_k(t)u(r,t) + \varphi_k(t)u(l,t)\right)dt + \int_0^t\int_{\Omega_i} fudxdt \\
=&\frac{1}{2}||u^0||^2_{\Omega_i} - \frac{2a^2\sqrt{z_0}}{2N+1}\sum_{k=1}^{N} a_k\left(||u(r,t) - (1-a_k)w_k(t)||^2_{[0,t]} + ||u(l,t) - (1-a_k)\varphi_k(t)||^2_{[0,t]}\right) \\
&\quad - \frac{a^2\sqrt{z_0}}{2N+1}\left(||u(r,t)||^2_{[0,t]} + ||u(l,t)||^2_{[0,t]}\right) + \int_0^t\int_{\Omega_i} fudxdt,
\end{aligned} \tag{3.7}$$

where $b_k = 2(1-a_k)/(2N+1)$. By using $2uf \le u^2 + f^2$ in (3.7), and denoting by $y(t) = ||u(x,t)||^2_{\Omega_i\times[0,t]}$, we arrive at

$$y'(t) \le y(t) + \phi(t).$$

The Gronwall's Lemma results in directly the desired estimate (3.1). □

3.2. Two-dimensional case

The purpose of this subsection is to prove the stability of systems (2.34).

Lemma 3.2. *Suppose that $u \in C^1[0,1]$. Then*

$$||u||^2_\infty \le ||u||^2_{[0,1]} + 2||u||_{[0,1]}||u_x||_{[0,1]}.$$

One can refer to [24] for the proof.

Theorem 3.2. *Assume that the initial values are smooth enough, then the Cauchy problem* (2.34) *has a unique weak solution and the following energy estimate holds:*

$$||u||^2_{\Omega_i\times[0,t]} \le e^t\left(||u^0||_{\Omega_i} + \int_0^t \phi(\tau)d\tau\right), \tag{3.8}$$

where $\phi(\tau)$ is given by

$$\phi(t) = ||u^0||^2_{\Omega_i} + Ca^2||g||^2_{\Gamma_0\times[0,t]} + ||f||^2_{\Omega_i\times[0,t]}. \tag{3.9}$$

Proof. By the same argument as the proof of Theorem 3.1, we can obtain the energy estimate. Only step (iii) need to be modified since two corner values appear and can be estimated by using Lemma 3.2. So we require a strong regularity for the datum at the corners, i.e., which can be bounded by a constant C. □

Remark 3.1 The conclusion of Theorem 3.2 can be extended to the reduced problems with ABCs (2.42)-(2.45), which is considered as a special case in Theorem 3.2 with $N = 1$.

4. Numerical Approximation and Examples

In the computational domain $[e,b]\times[c,d]$, let $\Delta x=(b-e)/I,\ \Delta y=(d-c)/J,\ \Delta t=T/L$ denote the spatial mesh sizes of variables x,y and the time size of time t, respectively, where $I,\ J,\ L$ are positive integers. Let the grid points and temporal mesh points be

$$x_i=e+i\Delta x,\quad y_j=c+j\Delta y,\quad t_\iota=\iota\Delta t$$

with $i=0,1,\cdots,I,\ j=0,1,\cdots,J,\ \ \iota=0,1,\cdots,L$. Denote the operators $D_+,\ D_-$ and D_0 by forward, backward and centered differences, respectively, $S_+,\ S_-$ and S_0 by forward, backward and centered sums, $\mathcal{I}$ by the identity operator; for example,

$$D_+^x u_i^\iota=(u_{i+1}^\iota-u_i^\iota)/\Delta x,\ S_+^t u_i^\iota=(u_i^{\iota+1}+u_i^\iota)/2,\ \mathcal{I}u_i^\iota=u_i^\iota.$$

Then we obtain the finite difference scheme of the heat equation

$$\left(D_+^t-a^2D_+^xD_-^xS_+^t-a^2D_+^yD_-^yS_+^t\right)u_{i,j}^\iota=f(x_i,y_j,t_{\iota+\frac{1}{2}}),$$

with $i=1,\cdots,I-1,\ j=1,\cdots,J-1,\ \iota=1,\cdots,L-1$ and the initial data $u_{i,j}^0=u^0\left(x_i,y_j,0\right)$. The boundary conditions are introduced to make the systems complete, and approximated by:

$$\begin{aligned}
&\frac{3u_{I,j}^\iota-4u_{I-1,j}^\iota+u_{I-2,j}^\iota}{2\Delta x}+\sqrt{z_0}\mathcal{I}u_{I,j}^\iota-\sqrt{z_0}\sum_{k=1}^N b_k w_{k,j}^\iota=0,\\
&(1-a_n)\,z_0S_+^tw_{n,j}^\iota+a_n\left(\frac{1}{a^2}D_+^t-D_+^yD_-^yS_+^t\right)w_{n,j}^\iota=z_0\mathcal{I}u_{I,j}^\iota-\left(\frac{1}{a^2}D_+^t-D_+^yD_-^yS_+^t\right)u_{I,j}^\iota,
\end{aligned}$$

where $j=1,2,\cdots,J-1$ and $n=1,2,\cdots,N.$ For corner points $(I,0)$ and (I,J), the strategies are given by

$$w_{n,j}^\iota=\frac{1}{\sqrt{z_0}N*b_n}\left(\frac{3u(I,j)^\iota-4u(I-1,j)^\iota+u(I-2,j)^\iota}{2\Delta x}+\sqrt{z_0}u^\iota(I,j)\right),\quad j=0\text{ or }J.$$

By restricting the discretization in the initial-boundary-value problem (2.20), we have

$$\left(D_+^t-a^2D_+^xD_-^xS_+^t\right)u_i^\iota=f\left(x_i,t_{\iota+\frac{1}{2}}\right),\qquad 0<\iota\le L,\ \ 1\le i<M.$$

The equations on the boundary points are approximated by

$$\begin{aligned}
&\frac{-3u_0^\iota+4u_1^\iota-u_2^\iota}{2\Delta x}-\sqrt{z_0}\mathcal{I}u_0^\iota+\sqrt{z_0}\sum_{k=1}^N b_k\varphi_k^\iota=0, && x=x_l,\\
&\left((1-a_k)z_0S_+^t+\frac{a_k}{a^2}D_+^t\right)\varphi_k^\iota-\left(z_0S_+^t+\frac{1}{a^2}D_+^t\right)u_0^\iota=0, && 1\le k\le N,\\
&\frac{3u_M^\iota-4u_{M-1}^\iota+u_{M-2}^\iota}{2\Delta x}-\sqrt{z_0}\mathcal{I}u_M^\iota+\sqrt{z_0}\sum_{k=1}^N b_kw_k^\iota=0, && x=x_r,\\
&\left((1-a_k)\,z_0S_+^t+\frac{a_k}{a^2}D_+^t\right)w_k^\iota-\left(z_0S_+^t+\frac{1}{a^2}D_+^t\right)u_M^\iota=0, && 1\le k\le N.
\end{aligned}$$

Example 4.1. In problem (2.20), let T $=1$, $x_l=-1,\ x_r=0,\ f(x,t)=u^0=0,\ u(x_l,t)=\operatorname{erfc}(\frac{1}{2\sqrt{t}})$ with

$$\operatorname{erfc}(x)=\frac{2}{\sqrt{\pi}}\int_x^\infty e^{-\lambda^2}d\lambda.$$

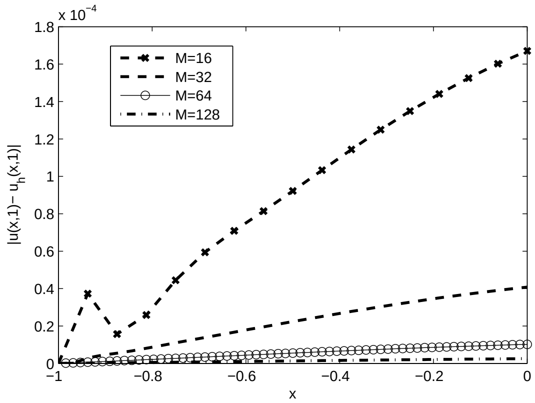

Fig. 4.1. Error $|u(x,1) - u_h(x,1)|$ with $N = 10$ on time line $t = 1$.

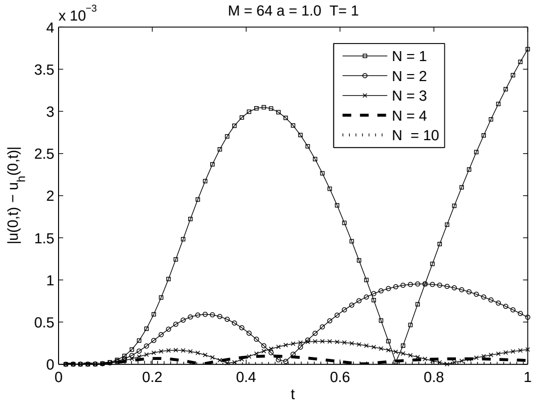

Fig. 4.2. The evolution of error $|u(0,t) - u_h(0,t)|$ for different N with $M = 64$.

Table 4.1: Error $|u(0,t) - u_h(0,t)|$ with different times and mesh sizes, (a, z_0, N)=(1.0, 1.0, 1.0).

	$M = 16$	order	$M = 32$	order	$M = 64$	order	$M = 128$	order
$t = 0.1875$	3.7596e-4	–	9.7266e-05	1.9506	2.37066e-05	2.0366	5.5784e-06	2.087
$t = 0.5625$	2.2603e-4	–	5.4063e-05	2.0638	1.37673e-05	1.9734	3.7925e-06	1.860
$t = 1$	1.6704e-4	–	4.0759e-05	2.0350	1.01853e-05	2.0006	2.5537e-06	1.996

Table 4.2: Error $\max_{0<t\leq 1} |u(0,t) - u_h(0,t)|$ with different N and z_0; $\Delta t = \Delta x = \frac{1}{1280}$.

$z_0 \setminus N$	1	3	5	7	10	20	40
0.5	7.9724e-3	8.5670e-4	1.5466e-4	3.7578e-5	6.0739e-6	1.2135e-7	6.5340e-8
1.0	3.7415e-3	2.5887e-4	3.2635e-5	5.9071e-6	7.7980e-7	6.8840e-8	6.5454e-8
10	3.0156e-3	1.1527e-5	1.2945e-7	6.4662e-8	6.5490e-8	6.5454e-8	6.5454e-8
20	1.6289e-2	4.6717e-5	2.2295e-7	6.5520e-8	6.5454e-8	6.5454e-8	6.5454e-8
50	4.2946e-2	4.3900e-3	2.0057e-4	2.8664e-6	6.5454e-8	6.5454e-8	6.5454e-8
100	6.5010e-2	1.5785e-2	2.7822e-3	7.2136e-6	6.5454e-8	6.5454e-8	6.5454e-8

The exact solution of the problem is

$$u(x,t) = \mathrm{erfc}(\frac{x+2}{2\sqrt{t}}). \tag{4.1}$$

In the calculation, let $\Delta t = \Delta x$ and $z_0 = 1.0$. Fig. 4.1 plots the absolute error $|u(x,1) - u_h(x,1)|$ with $N = 10,\ M = 16, 32, 64, 128$. Fig. 4.2 shows the evolution of the absolute error $|u(0,t) - u_h(0,t)|$ on the boundary point with $a = 1.0$, $M = 64$ and different parameters N.

One can see that the error on boundary point decreases quickly when M and N are endowed with larger and larger values. Table 4.1 presents the error in L_∞-norm with $M = 16,\ 32,\ 64,\ 128$ at different times.

From Table 4.1, it can be seen that the absolute error $|u(0,t) - u_h(0,t)|$ in L_∞-norm has the second-order convergence rate with respect to $h = \Delta x$, i.e., there exists a constant C such that

$$||u(0,t) - u_h(0,t)||_\infty \approx Ch^2.$$

We now investigate the error $\max_{0<t\le 1} |u(0,t) - u_h(0,t)|$ with different parameters z_0 and N. Taking $\Delta t = \Delta x = \frac{1}{1280}$, some results are shown in Table 4.2.

From Table 4.2, one can see that the parameter z_0 has an important influence on the effectiveness of the high-order ABCs. For the adaptive choice of the parameter, one can refer to [35, 37, 38] and references therein.

Example 4.2. To show the tractability and effectiveness of the method, we let $T = 0.9$, $f(x,y,t) = 0,\ u^0 = u(x,y,0)$,

$$g(x,y,t)|_\Gamma = \frac{1}{4a^2\pi\,(t+t_0)} \exp\left(-\frac{x^2+y^2}{4a^2\,(t+t_0)}\right)\Big|_\Gamma .$$

The exact solution of the system (2.34) with the above initial-value and boundary condition is

$$u\,(x,y,t) = \frac{1}{4a^2\pi\,(t+t_0)} \exp\left(-\frac{x^2+y^2}{4a^2\,(t+t_0)}\right).$$

We choose $e = c = -2,\ b = d = 2$ and $a = 1$ and let $\Delta t = \Delta x = \Delta y,\ t_0 = 0.1$. Without loss of generality, we take $z_0 = 1.0$ in the following calculation. Denote by the L_1-norm

$$L_1 = \frac{1}{(I+1)(J+1)(L+1)} \sum_{n=0}^{L}\sum_{i=0}^{I}\sum_{j=0}^{J} \left|u(x_i,y_j,t_n) - u_{ij}^n\right| .$$

Firstly we check the influence of truncated numbers N on the ABCs. Fig. 4.3 shows the evolution of the L_1-norm for different truncated number N with mesh size 128×128. Fig. 4.4 presents the evolution of the L_1-norm under different meshes when truncated number N chosen to 5.

Table 4.3: L_1-norms and convergence order for different meshes and N.

	32×32	order	64×64	order	128×128	order	256×256	order
$N=1$	7.338e-4	–	2.428e-4	1.706	9.804e-5	1.198	6.869e-5	0.513
$N=3$	7.153e-4	–	1.885e-4	1.924	5.050e-5	1.901	1.614e-5	1.645
$N=10$	7.158e-4	–	1.891e-4	1.921	4.988e-5	1.922	1.419e-5	1.813

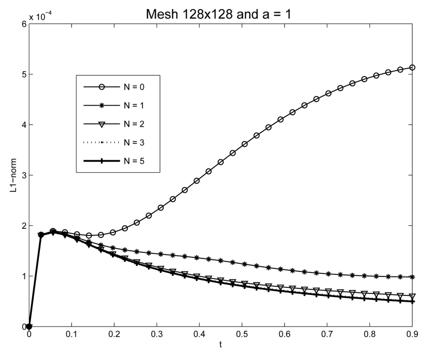

Fig. 4.3. The evolution of L_1-norm with different N at mesh 128×128.

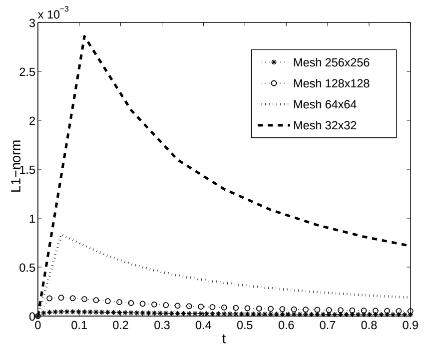

Fig. 4.4. Comparison of the evolution of L_1-norm at different meshes and $N = 10$.

Table 4.3 presents the L_1-error and convergence order with mesh sizes from $I \times J = 32 \times 32$ to 256×256 and different N. It can be seen that the error in L_1-norm decreases with truncated number N growing and trends to the second-order convergence rate. Despite L_1-norm plays an important role in testing the efficiency of the method, sometimes one need to check the maximum value of point errors when the mesh is refined or N is chosen different values. The infinity norm L_∞ for the fixed time level l is defined by

$$L_\infty = \max_{i,j} |u(x_i, y_j, t_l) - u_{ij}^l|, \quad 0 \le i \le I \ , \ 0 \le j \le J.$$

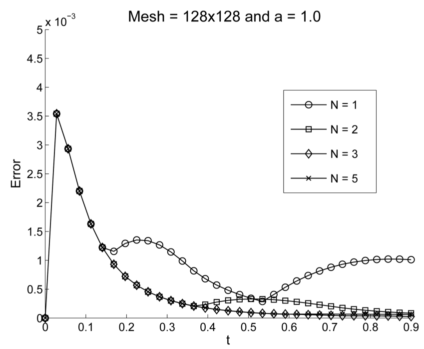

Fig. 4.5. The evolution of L_∞ with different N and mesh = 128×128.

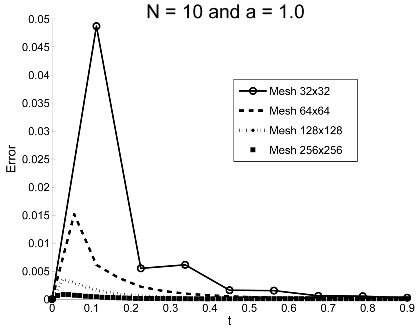

Fig. 4.6. The evolution of L_∞ with different meshes and $N = 10$.

Fig. 4.5 shows the evolution of global L_∞-norm for different truncated number N with mesh size 128×128. One can see that the error in $L_\infty-$norm deceases with N increasing. Fig. 4.6 presents the L_∞-norm under different mesh sizes at each time line when N is fixed with 10.

5. Conclusion

We have obtained the high-order artificial boundary conditions for the heat equation and proved that the reduced initial-boundary-value problems are stable. This approach provides the considerable insight into the construction of the local ABCs for linear equations. We expect that these results would be useful for the numerical study on a family of nonlinear PDEs.

Acknowledgments. This research is supported in part by RGC of Hong Kong and FRG of Hong Kong Baptist University. We thank the referees for their careful reading of the paper and for suggestions that led to an improved version of the paper.

References

[1] X. Antoine, A. Arnold, C. Besse, M. Ehrhardt, and A. Schädle, A Review of Transparent and Artificial Boundary Conditions Techniques for Linear and Nonlinear Schrödinger Equations, *Commun. Comput. Phys.*, **4**:4 (2008), 729-796.

[2] A. Bamberger, B. Engquist, L. Halpern, and P. Joly, Higher order paraxial wave equation approximations in heterogeneous media, *SIAM J. Appl. Math.*, **48**:1 (1988), 129-154.

[3] J. Bérenger, A perfectly matched layer for the absorption of electromagnetic waves, *J. Comput. Phys.*, **114** (1994), 185-200.

[4] H. Brunner, X. Wu, and J. Zhang, Computational solution of blow-up problems for semilinear parabolic PDEs on unbounded problem, *SIAM J. Sci. Comput.* **31**(6)(2010), 4478-4496.

[5] F. Collino, High order absorbing boundary conditions for wave propagation models: Straight line boundary and corner cases, in: R.Kleinman, et al. (Eds.), Proceedings of the Second International Conference on Mathematical and Numerical Aspects of Wave Propagation, *SIAM, Delaware*, (1993) 161-171.

[6] B. Engquist and A. Majda, Absorbing boundary conditions for the numerical simulation of waves, *Math. Comput.*, **31** (1977), 629-651.

[7] K. Feng and D. Yu, Canonical integral equations of elliptic boundary value problems and their numerical solutions, *Proc. of China-France Symposium on Finite Element Methods*, Feng, K., Lions, J.L. (Eds.), Science Press, 1983, 211-252.

[8] D. Givoli, Finite element analysis of heat problems in unbounded domains, In Numerical Methods in Thermal Problems, Vol. VI, (Edited by R.W. Lewis and K. Morgen), Part **2** (1989), 1094-1104, *Pineridge Press*, Swansea, U.K.

[9] D. Givoli, High-order local non-reflecting boundary conditions: a review, *Wave Motion*, **39** (2004), 319-326.

[10] D. Givoli and B. Neta, High-order non-reflecting boundary scheme for time-dependent waves, *J. Comput. Phys.*, **186** (2003), 24-46.

[11] L. Greengard and P. Lin, On the numerical solution of the heat equation in unbounded domains (Part I), *Tech. Note* 98-002, Courant Mathematics and Computing Laboratory, New York University, (1998).

[12] M. Grote and J. Keller, On nonreflecting boundary conditions, *J. Comput. Phys.*, **122** (1995), 231-243.

[13] T. Hagstrom, M. de Castro, D. Givoli, and D. Tsemach, Local high order absorbing boundary conditions for time-dependent waves in guides, *J. Comput. Acoust.*, **15** (2007), 1-22.

[14] T. Hagstrom, S. Hariharan, and D. Thompson, High-order radiation boundary conditions for the convective wave equation in exterior domains, *SIAM J. Sci. Comput.*, **25** (2003), 1088-1101.

[15] T. Hagstrom, A. Mar-Or, and D. Givoli, High-order local absorbing conditions for the wave equation: extensions and improvements, *J. Comput. Phys.*, **227** (2008), 3322-3357.

[16] T. Hagstrom and T. Warburton, A new auxiliary variable formulation of high-order local radiation boundary conditions: corner compatibility conditions and extensions to first order systems, *Wave Motion*, **39** (2004), 327-338.

[17] H. Han, The artificail boundary method - numerical solutions of partial differential equations in unbounded domains, in: T. Li, P. Zhang(Eds.), *Frontiers and Prospents of Contemporary Applied Mathematics*, Higher Education Press and World Scientific, 33-66 (2006).

[18] H. Han and Z. Huang, Exact and approximating boundary conditions for the parabolic problems on unbounded domains, *Comput. Math. Appl.*, **44** (2002), 655-666.

[19] H. Han and Z. Huang, A class of artificial boundary conditions for heat equation in unbounded domains, *Comput. Math. Appl.*, **43** (2002), 889-900.

[20] H. Han, J. Lu, and W. Bao, A discrete artificial boundary condition for steady incompressible viscous flows in a no-slip channel using a fast iterative method, *J. Comput. Phys.*, **114** (1994), 201-208.

[21] H. Han and X. Wu, Approximation of infinite boundary condition and its applications to finite element methods, *J. Comput. Math.*, **3** (1985), 179-192.

[22] H. Han and D. Yin, Numerical solutions of parabolic problems on unbounded 3-D spatial domain, *J. Comput. Math.*, **23** (2005), 449-462.

[23] J. Keller and D. Givoli, Exact nonreflecting boundary conditions, *J. Comput. Phys.*, **82** (1989), 172-192.

[24] H. Kreiss and J. Lorenz, Initial boundary value problems and the Navier-Stokes equations, *III. Series: Pure and applied mathematics Academic Press*, Volume **136**, 1989.

[25] J. Li and L. Greengard, On the numerical solution of the heat equation I: Fast solvers in free space, *J. Comput. Phys.*, **226** (2007), 1891-1901.

[26] E. Lindmann, Free-boundary conditions for the time dependent wave equation, *J. Comput. Phys.*, **18** (1975), 66-78.

[27] L. Menza, Absorbing boundary conditions on a hypersurface for the Schrödinger equation in a half space, *Appl. Math. Lett.*, **9** (1996), 55-59.

[28] L. Menza, Transparent and absorbing boundary conditions for the Schrödinger equation in a bounded domain, *Numer. Func. Anal. Opt.*, **18** (1997), 759-775.

[29] J. Strain, Fast adaptive methods for the free-space heat equation, *SIAM J. Sci. Comput.*, **15** (1994), 185-206.

[30] J. Szeftel, Design of absorbing boundary conditions for Schrödinger equations in $\mathbb{R}^d$, *SIAM J.*

Numer. Anal., **42** (2004), 1527-1551.

[31] J. Szeftel, Absorbing boundary conditions for one-dimensional nonlinear Schrödinger equations, *Numer. Math.*, **104** (2006), 103-127.

[32] X. Wu and Z. Sun, Convergence of difference scheme for heat equation in unbounded domains using artificial boundary conditions, *Appl. Numer. Math.*, **50** (2004), 261-277.

[33] X. Wu, J. Zhang, Artificial boundary method for two-dimensional Burgers' equation, *Comput. Math. Appl.*, **56**:1 (2008), 242-256.

[34] Z. Xu, H. Han and X. Wu, Numerical method for the deterministic Kardar-Parisi-Zhang equation in unbounded domains, *Commun. Comput. Phys.*, **1** (2006), 479-493.

[35] Z. Xu, H. Han, and X. Wu, Adaptive absorbing boundary conditions for schrodinger-type equations: application to nonlinear and multi-dimensional problems, *J. Comput. Phys.*, **225** (2007), 1577-1589.

[36] D. Yu, Approximation of boundary conditions at infinity for a harmonic equation, *J. Comput. Math.*, **3** (1985), 219-227.

[37] J. Zhang, Z. Xu, and X. Wu, Unified approach to spit absorbing boundary conditions for nonlinear Schrödinger equations, *Phys. Rev. E*, **78** (2008), 026709.

[38] J. Zhang, Z. Xu, and X. Wu, Unified approach to split absorbing boundary conditions for nonlinear Schrodinger equations: Two-dimensional case, *Phys. Rev. E*, **79** (2009), 046711.

[39] C. Zheng, Exact nonreflecting boundary conditions for one-dimensional cubic nonlinear Schrödinger equations, *J. Comput. Phys.*, **215** (2006), 552-565.

[40] C. Zheng, A perfectly matched layer approach to the nonlinear Schrödinger wave equations, *J. Comput. Phys.*, **227** (2007), 537-556.

[41] C. Zheng, Approximation, stability and fast evaluation of exact artificial boundary condition for the one-dimensional heat equation, *J. Comput. Math.*, **25** (2007), 730-745.

[42] C. Zheng, An exact absorbing boundary condition for the Schröinger equation with sinusoidal potentials at infinity, *Commun. Comput. Phys.*, **3** (2008), 641-658.